The Journal of Physical Chemistry

 VOLUME 99, NUMBER 21, MAY 25, 1995

LETTERS

Excess Energy-Dependent Photodissociation Probabilities for O_2^- in Water Clusters: $O_2^-\cdot(H_2O)_n$, $1 \leq n \leq 33$

David J. Lavrich, Mark A. Buntine,† David Serxner, and Mark A. Johnson*,‡

Sterling Chemistry Laboratory, Yale University, New Haven, Connecticut 06511

Received: March 10, 1995®

We report the branching ratios, ϕ, for photodissociation of O_2^- in water clusters, $O_2^-\cdot(H_2O)_n$, as a function of excess energy [over the bond energy, $E_{excess} = h\nu - D_o(O_2^-)$] and cluster size, $1 \leq n \leq 33$. The two-dimensional $\phi(E_{excess}, n)$ "dissociation" surface is generated from a series of measurements over the range $0 \leq E_{excess} \leq 1.8$ eV and displays features attributable to attractive forces at small E_{excess} and repulsive interactions at high E_{excess}. This $\phi(E_{excess}, n)$ surface is essentially independent of cluster size in the range $18 \leq n \leq 33$, where all clusters are characterized by a single $\phi(E_{excess})$ curve. Similarly, $\phi(E_{excess}, n)$ becomes independent of E_{excess} at high E_{excess} (≥ 1 eV) with a characteristic $\phi(n)$ dependence. At *both* large E_{excess} and large n, $\phi(E_{excess}, n)$ displays a plateau at about 0.70 which is very weakly dependent on both E_{excess} and n. We interpret the shape of the surface in the context of a model recently developed by Apkarian and co-workers (*J. Phys. Chem.* **1994**, 98, 7966) to explain the excess energy-dependent dissociation yields for small molecules in rare-gas matrices.

I. Introduction

One of the most basic effects of a solvent on a chemical reaction is the moderation of the kinetic energy of the atoms as they experience the strong local forces at play on a reactive potential-energy surface. The important features of the problem are displayed in the photodissociation of a diatomic molecule in a medium. Over the past 20 years, a great deal of work has been directed at understanding the geminate recombination or "cage" dynamics of simple species such as I_2 photodissociated in solutiton.[1-5] These studies have been extended to diatomics in clusters by Lineberger and co-workers,[6] who established the size dependence of the geminant recombination quantum yield for photodissociated Br_2^- and I_2^- in CO_2 clusters. Lineberger[7,8] and Zewail[9,10] further characterized the time scale for recovery of the I_2^- and I_2 absorptions in CO_2 and He clusters, respectively, using ultrafast pump–probe methodology. A third class of experiments probed the dependence of the dissociation yield as a function of the initial energy imparted to the species above the bond dissociation energy, E_{excess}. Schwentner[11,12] and Apkarian[13] have reported $\phi(E_{excess})$ for the photodissociation of H_2O and H_2S, respectively, in rare-gas matrices. The solid-state experiments are interesting in that the sigmoidal shape of the $\phi(E_{excess})$ function has been used to extract mechanical parameters such as the height of the potential barrier controlling the atom escape from one octahedral site to the next.

While this $\phi(E_{excess})$ function should be directly comparable to measurements carried out in clusters, there are at present only data available for the dependence of ϕ on cluster size at a few selected wavelengths. In this paper, we report the shape of $\phi(E_{excess})$ for the case of photodissociation of O_2^- within size-selected $(H_2O)_n$ clusters as a function of *both* initial kinetic energy and cluster size. To visualize this rather large data set,

† Present address: Department of Chemistry, University of Adelaide, Adelaide, S.A. 5005, Australia.
‡ Camille and Henry Dreyfus Teacher–Scholar.
® Abstract published in *Advance ACS Abstracts,* May 1, 1995.

0022-3654/95/2099-8453$09.00/0

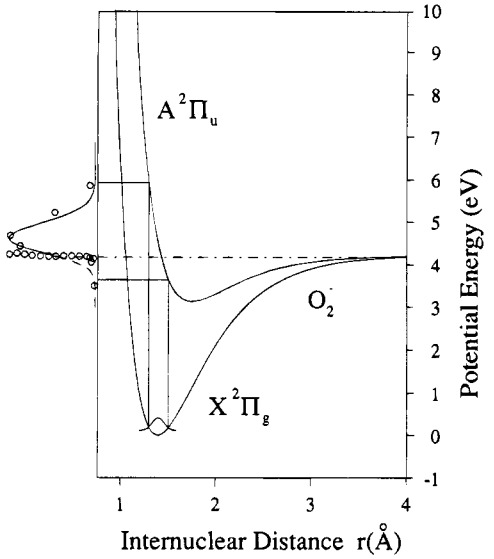

Figure 1. Potential-energy curves for the $X^2\Pi_g$ and $A^2\Pi_u$ states of O_2^-, with the O^- photofragment action spectrum displayed along the ordinate.

we introduce the two-dimensional *dissociation surface*, $\phi(E_{excess}, n)$, which encodes the evolution of the atom-stopping power from the bare species through the cluster regime toward the bulk. We find that the $\phi(E_{excess}, n)$ function displays two asymptotic regions: one at larger cluster sizes ($18 < n < 33$), in which there is an n-independent evolution of ϕ *vs* E_{excess}, and another at high E_{excess}, where ϕ *vs* n is only weakly dependent on E_{excess}. The origin of the asymptotic behaviors is traced to a structural signature of the clusters which is interrogated by the repulsive nature of the high-energy atom–solvent collision. Below these asymptotes, we interpret the region of rapidly varying $\phi(E_{excess}, n)$ in the context of a potential trapping model suggested by Apkarian and co-workers[13] to account for dissociation yields in rare-gas matrices.

II. Review of O_2^- Spectroscopy

We have recently reported the observation of the ultraviolet $A^2\Pi_u \leftarrow X^2\Pi_g$ dissociative electronic transition both in bare O_2^- and in O_2^- solvated in water clusters.[14] The potential curves for the superoxide anion are shown schematically in Figure 1. The relative displacement of the curves indicates that, in the Franck–Condon region for absorption from $X^2\Pi_u$ ($v = 0$), the maximum photodissociation cross section occurs for excitation at the inner repulsive wall of the $A^2\Pi_u$ state such that the dissociating atoms are just at the dissociation threshold after traversing a shallow minimum [$D_o(A^2\Pi_u) \sim 1$ eV]. This situation allows the kinetic energy of the ejected atoms to be prepared over the range 0–2 eV within the main part of the (truncated) Gaussian-shaped O^- action spectrum, displayed along the vertical axis in Figure 1. The region of the A state excited from X ($v = 0$) is, of course, well into the electron continuum of $O_2 + e^-$ since the electron binding energy of O_2^- is only 0.45 eV.[15] The A state is relatively stable with respect to autodetachment, however, since electron ejection from the primarily $(\pi_u^3\pi_g^4)$ configuration of the A state is a two-electron process to create the ground-state $(\pi_u^4\pi_g^2)$ configuration of O_2.[16] Photoelectron spectra[17] of the $O_2^-{\cdot}H_2O$ complex indicate that the characteristic electronic pattern of the O_2^- core ion is indeed intact in the cluster system, although the O_2 vibrational features are washed out in this tightly bound complex ($D_o = 0.78$ eV). The fact that O_2^- forms the charge-localized core in the binary complex as well as in small water clusters is not surprising,

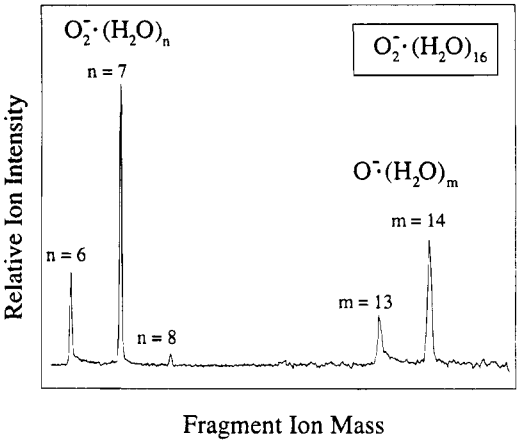

Figure 2. Anionic fragment distribution from photodissociation of $O_2^-{\cdot}(H_2O)_{16}$ at 266 nm ($E_{excess} = 0.57$ eV). The distribution consists of two classes of fragments: $O_2^-{\cdot}(H_2O)_n$, corresponding to recombination of oxygen atoms, and $O^-{\cdot}(H_2O)_m$, resulting from escape of an oxygen atom in addition to water monomer evaporations.

since the superoxide anion is well-known as an important entity in aqueous chemistry[18] and has been characterized by ESR as charge-localized in the bulk,[19] with a UV absorption consistent with the persistence of the $A \leftarrow X$ intramolecular transition in the aqueous anion.[20]

III. Experimental Section

Mass-selected clusters of $O_2^-{\cdot}(H_2O)_n$, $0 \le n \le 33$, are photodissociated in a standard tandem time-of-flight mass spectrometer in which the daughter ions are dispersed with a reflectron.[21] The $O_2^-{\cdot}(H_2O)_n$ parent ion distribution is created by electron transfer from $(H_2O)_n^-$ to O_2 after intersection of a 1.5-kV electron beam at the throat of a supersonic expansion containing oxygen saturated with water vapor. Photoexcitation in the range 200–300 nm is carried out with a frequency-doubled, optical parametric oscillator (Spectra Physics MOPO 710) in addition to the fourth and fifth harmonics of a Nd:YAG laser (Spectra Physics GCR-4.)

Photodissociation of $O_2^-{\cdot}(H_2O)_n$ yields two classes of fragments corresponding to two different loss mechanisms. Figure 2 presents a typical photofragment distribution from photoexcitation of $O_2^-{\cdot}(H_2O)_{16}$. The photofragment classes are easily identified according to the number of water molecules evaporated. The heavy distribution results from loss of 2 or 3 water monomers, while the lighter class results from ejection of 9 or 10 water monomers. Within each class, the distributions are rather narrow (about 1.5 monomer units wide). Note that the lightest fragments in each class have a pronounced asymmetry toward longer flight time arising from slow decay of the penultimate fragment in the reflection, indicating a fragmentation rate for the final evaporation on the order of 10^5 s^{-1}.

The two classes of photofragments result from two different loss mechanisms:

$$O_2^-{\cdot}(H_2O)_n + h\nu \rightarrow O^-{\cdot}(H_2O)_{n-m} + mH_2O + O \quad \langle m \rangle = 2.4 \quad (1a)$$

$$O_2^-{\cdot}(H_2O)_n + h\nu \rightarrow O_2^-{\cdot}(H_2O)_{n-p} + pH_2O \quad \langle p \rangle = 10.0 \quad (1b)$$

where $\langle m \rangle$ and $\langle p \rangle$ denote the average number of water molecules lost in each channel. The heavier fragment corresponds to loss of an oxygen atom in addition to water monomers, while the lighter fragments have a mass corresponding to loss of only

water molecules from the parent. The appearance of two-photon photofragments at high laser fluence indicates that the lighter class of photofragments in Figure 2 indeed corresponds to reformation of ground-state O_2^- (after dissociation) with internal energy near the bottom of the potential. These secondary fragments arise from photodissociation of the [mostly $(O_2^-\cdot(H_2O)_7$] primary fragments with a second photon, yielding a secondary fragment distribution that is quite similar to that of the $O_2^-\cdot(H_2O)_7$ cluster selected from the parent distribution. The disparity in evaporation yields between the two classes [(1a) *vs* (1b)] occurs since, once O_2^- is dissociated, only excess energies above the O_2^- bond energy contribute to evaporation, while all of the photon energy is available when O_2^- is recombined after photodissociation. Thus, the difference in the number of waters lost in each class [$(\langle p\rangle - \langle m\rangle) \sim 7.6$] is approximately the O_2^- bond energy *in the cluster* in units of the average monomer evaporation energy, ΔE_{evap}. We can estimate ΔE_{evap} from process (1b) as $\Delta E_{evap} \approx h\nu/10 \approx 0.47$ eV to obtain an approximate value for $D_o(O_2^-)$ of ~3.5 eV, somewhat smaller than the gas-phase value of 4.09 eV. This difference in $D_o(O_2^-)$ is expected from the differential solvation energy of O^- relative to O_2^-. The observed difference is comparable to the difference in single-ion hydration energies of similar ions [$\Delta H_{hyd}(F^-) = 4.90$ eV *vs* $\Delta H_{hyd}(O_2^-) \approx 4.36$ eV][22] but somewhat larger than the value derived from evaporative charge-transfer reactions leading to $O^-\cdot(H_2O)_n$ and $O_2^-\cdot(H_2O)_n$.[23,24]

We have also carried out these studies using $O_2^-\cdot(D_2O)_n$ clusters and have found results that are indistinguishable from those obtained from $O_2^-\cdot(H_2O)_n$ clusters. The mass spectra of the $O_2^-\cdot(D_2O)_n$ clusters allow us to unambiguously establish that the heavy fragments have $O^-\cdot(D_2O)_n$ stoichiometry for parents $n \leq 20$, indicating that the oxygen atom has indeed escaped from the cluster. At larger parents, it is possible that the heavy fragments could also have $O_2^-\cdot(H_2O)_k$ stoichiometry so long as the O^- and O fragments are separated within the cluster, since dissociation is readily distinguished from recombination based upon the number of evaporation events. Retention of the (^{3}P) oxygen atom in the larger clusters appears unlikely, however, since once it is separated from O^-, it is the most weakly bound entity in the cluster and should be preferentially ejected relative to the evaporation of water monomers.

We remark that for $O_2^-\cdot(D_2O)_n$, $n \leq 20$, the fragments are dispersed with sufficient resolution to reveal a very small class of fragments (at most, less than 4% of the total fragmentation intensity), resulting from proton-transfer and hydrogen-transfer reactions resulting in OD^- and O_2D^- based clusters, respectively. Since they represent minor channels, we postpone a full discussion of the intracluster reactions to a later paper.

IV. Results and Discussion

The O_2^- dissociation probability is determined from the ratio of the peak intensities of the heavier fragments relative to the total photofragmentation yield:

$$\phi(E_{excess}, n) = \frac{I(O^-)}{I(O_2^-) + I(O^-)} \qquad (2)$$

where $I(O_2^-)$ and $I(O^-)$ denote the total ion counts appearing in the light and heavy distributions, respectively. The arguments of $\phi(E_{excess}, n)$ remind us that we are monitoring the shape of $\phi(E_{excess}, n)$ as a function of excess energy, E_{excess} (defined as $h\nu - D_o$), and cluster size n. The language "oxygen atom escape" is, of course, potentially misleading since the dissociating $[O{-}O]^-$ entity is charge-delocalized over both oxygen atoms

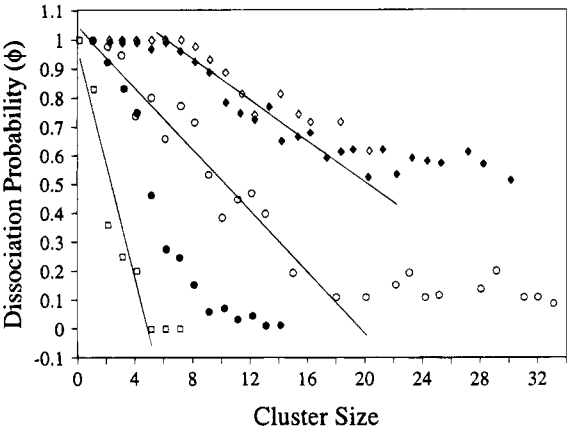

Figure 3. Oxygen atom dissociation probability, $\phi(E_{excess}, n)$, displayed as a function of cluster size at several excess energies (□ = 0.01 eV, ● = 0.34 eV, ○ = 0.57 eV, ♦ = 1.08 eV, ◇ = 1.73 eV). Excess energy is defined as $E_{excess} = h\nu - D_o$, where $D_o = 4.09$ eV for the gas-phase species.

until the asymmetry of the solvent molecules induces charge localization.[25] It is presently unclear whether the energy transfer from dissociating O_2^- to the solvent occurs in the charge-localized or charge-delocalized regimes.[26] Energetic considerations dictate, however, that the ultimate fragment must be the neutral O atom rather than O^-, since the solvation energy of O^- with even a few solvent molecules is much larger than that of O neutral (recall that O(^{3}P) is quite unreactive with H_2O in aqueous media due to a high barrier $E_a \approx 0.401$ eV).[27,28]

Figure 3 presents a summary of the dissociation probabilities, $\phi(E_{excess}, n)$, at several excess energies. As might be expected, for fixed excess energy, ϕ decreases with increasing cluster size as additional water molecules serve to slow down and finally stop the primary photofragments. The shape of this n-dependence is generally sigmoidal, displaying a prolonged linear region where each water is progressively more effective in arresting dissociation, as observed previously by the Boulder group.[6] For $E_{excess} < 0.5$ eV, $\phi(E_{excess}, n)$ evolves continuously from unity to zero (complete dissociation to complete recombination). The curve for $E_{excess} = 0.57$ eV is curious, however, in that the dissociation yield falls linearly in the range $0 < n < 18$ and then flattens out at a nonzero value, remaining constant at $\phi \approx 0.1$ for $18 \leq n \leq 33$. *Increasing solvation above $n \approx 18$ does not enhance the recombination yield!* While the dissociation yield is essentially independent of cluster size above 18, the *value* of ϕ in this asymptotic regime still depends on the initial excitation energy such that at $E_{excess} = 1.08$ eV, $\phi(E_{excess}, n)$ reaches a higher asymptotic value of ~0.6.

It is useful when considering $\phi(E_{excess}, n)$ to plot the two-dimensional surface in order to highlight the asymptotic regimes. We have therefore constructed the $\phi(E_{excess}, n)$ surface by interpolation of the data displayed in Figure 3, with the result displayed in Figure 4. Inspection of this surface indicates that there is a region for small values of n and E_{excess} where $\phi(E_{excess}, n)$ is changing rapidly in both coordinates. The asymptotic behavior at high n is clearly seen as a ramp along the E_{excess} axis, with a similar asymptotic sheet at high E_{excess} along the cluster size axis. Both asymptotes merge at high n and high E_{excess} to a plateau where $\phi \approx 0.70$ is independent of *both* E_{excess} and n.

Several features of the "dissociation surface" shown in Figure 4 correlate to the behavior observed for the photodissociation of small molecules in rare-gas matrices. For example, Schwentner and co-workers[11,12] have monitored the probability for hydrogen atom escape from octahedral sites upon photodissociation of

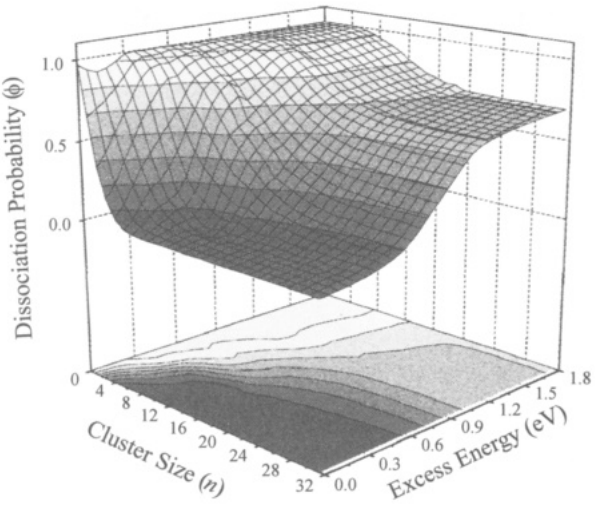

Figure 4. Upper trace shows the dissociation surface, $\phi(E_{excess}, n)$, as a function of E_{excess}, and n, constructed from a 2-D spline of the raw data. Contours of $\phi(E_{excess}, n)$ are shown on the (E_{excess}, n) plane below the caging surface at intervals of 0.125 eV, revealing their parallel nature at $E_{excess} \leq 0.6$ eV and $n \leq 10$.

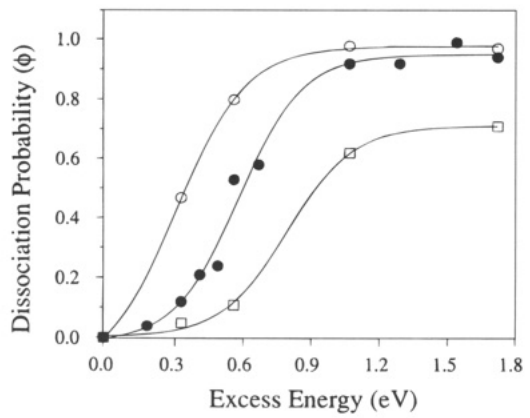

Figure 5. Oxygen atom dissociation probability, $\phi(E_{excess}, n)$, as a function of E_{excess} at three cluster sizes (○ = $O_2^-\cdot(H_2O)_5$, ● = $O_2^-\cdot(H_2O)_9$, □ = $O_2^-\cdot(H_2O)_{18}$). The spline fits through the data are eye-guides.

H_2O in solid xenon, krypton, and argon. These authors report $\phi(E_{excess})$, which corresponds to the bulk limit of cluster determinations of $\phi(E_{excess}, n)$. For the case of photodissociation in Xe, $\phi(E_{excess})$ is sigmoidal in shape with an onset increasing as $(E - E_{th})^2$, where E_{th} is the minimum energy required for hydrogen to pass through the Xe host lattice into the next octahedral site. To compare with the solid-state studies, we plot slices of the $\phi(E_{excess}, n)$ surface at fixed n for $n = 5$, 9, and 18 in Figure 5. These curves are quite similar in shape to the matrix results where the "threshold" increases while the dissociation yield drops at larger cluster sizes.

Apkarian[13] has treated the general shape of $\phi(E_{excess})$ with a simple model in which the guest chromophore is assumed to be randomly oriented in the host lattice and the photoejected atoms must pass over an additional potential barrier (in addition to the dissociation energy of the bare molecule), defined by the van der Waals radii of the matrix atoms, in order to drop into a neighboring lattice site. In this model, the minimum in the barrier will be in the center of the unit cell with increasing energy toward any of the host atoms. The permanent dissociation probability is then controlled by the area circumscribed by the contour accessed by a given E_{excess} above this minimum, which is found to be roughly linear in E_{excess} near threshold for a rigid lattice. (This is a general feature of a spherical potential; the area of a circle obtained by intersecting a plane with a sphere grows linearly with the distance that the plane penetrates into the sphere. Given a sphere of radius R, a plane through the sphere at a distance E to a parallel plane tangential to the surface intersects a circular area, $A = \pi(2RE - E^2)$. As the distance E is increased from the surface ($E = 0$) toward the center of the sphere ($E = R$), the area A increases approximately linearly in the regime of small E.) Apkarian[13] recovers the sigmoidal shape by including fluctuations in the trapping potential due to the zero-point motion of the lattice.

Thus, the general shape of $\phi(E_{excess})$ is expected to have an onset at finite E_{excess}, with a value related to the threshold for dissociation, and display a roughly linear increase toward some asymptotic value. The three curves in Figure 5 clearly show an increasingly delayed threshold for larger clusters. In the soft barrier penetration model, these shapes reflect an increase in the potential as more solvent molecules envelop the O_2^-, which in turn narrows the dissociation window, requiring more excess energy to escape. This trade-off region is easily seen in the contour plot at the bottom of Figure 4, where the dense series of parallel contours project out from the origin at roughly a 45° angle. The similarity in slopes in the dependence of excess energy on cluster size for constant ϕ is interesting, indicating that the "stopping power" for the solvent molecules (defined by this slope) has a value of about 0.1 eV/molecule. This is the regime Lineberger and co-workers[6] refer to as the "attractive caging" regime.

Larger clusters ($n > 18$ or so) do not obey this constant-energy loss/molecule rule as evidenced by the contours becoming independent of n. In fact, the asymptotic, sigmoidal shape of $\phi(E_{excess})$ at high n appears to indicate that the local environment of O_2^- is stabilized above $n \approx 20$. Another aspect of the $\phi(E_{excess}, n)$ surface at high n and E_{excess} is the plateau region where $\phi \approx 0.70$. The finite, nonunity value at high energy can be traced to the momentum transfer for head-on collisions between an oxygen atom ($m = 16$) and a water molecule ($m = 18$). A direct repulsive encounter with a solvent molecule will cause a reversal in the recoil velocity with loss of about half the initially imparted energy. These direct hits will then stop even a very rapidly escaping atom with a probability related to the cross section presented by the solvent "targets". In this context, the asymptotic n dependence and the finite ($\phi \approx 0.70$) plateau appear related; both suggest that the local structure is established around $n = 20$ and the $\phi(E_{excess})$ curve for high n indicates the action function for dissociation from this structure. While it can be argued that the relative n-independence from 18 to 33 is traceable to the fact that the second shell is farther away so that it takes many more molecules to effectively increase the "thickness" of the cluster wall, it is nonetheless surprising that we do not see a gradual increase in $\phi(E_{excess}, n)$ toward a second solvation shell asymptote. Alternatively, if there is a potential *barrier* to escape from the first shell, the second shell could serve to stop the escaping O atom with sufficient energy loss that it cannot recross the barrier to re-enter the first shell and recombine with the O^-. Since our experiment monitors dissociation rather than oxygen escape at the larger sizes (see discussion in Section III), we cannot determine whether the second shell is indeed incrementally slowing the oxygen atom; we can only show that recombination does not occur as a consequence of this slowing.

In this regard, it is important to establish exactly how water clusters grow around a so-called "core" anion. Recent calculations by Berkowitz[29,30] and Jorgensen,[31] for example, indicate that the strong, directional hydrogen-bonding network in water causes asymmetric growth of the solvent around the anion, with the anion located closer to the surface than expected for more

weakly interacting solvents such as CO_2. Garrett[32] has modeled the vertical electron-binding energies of $I^-\cdot(H_2O)_{n=1-15}$ clusters (determined by Cheshnovsky[33] with photoelectron spectroscopy) and has shown that the lowest energy configurations for these clusters have surface-solvated anions. On the other hand, Bowen[34] has obtained photoelectron spectra of $O^-\cdot(Ar)_{n=1-26}$ clusters and argues that these data are most consistent with a shell closing at $n = 12$, corresponding to an icosahedral structure. In light of the present uncertainty about the location of the anions within clusters, it would be useful to determine the shape of the $\phi(E_{excess}, n)$ surface for more weakly bound systems to see if its topology can provide a signature of the arrangement of solvent molecules around an anion.

Acknowledgment. We thank the National Science Foundation for support of this work under NSF 9207894 and helpful discussions with Prof. A. Apkarian, who provided us with a preprint of ref 13.

References and Notes

(1) Harris, A. L.; Brown, J. K.; Harris, C. B. *Annu. Rev. Phys. Chem.* **1988**, *39*, 341.
(2) Alan, N.; Abdul-Haj, N. A.; Kelley, D. F. *J. Chem. Phys.* **1986**, *84*, 1335.
(3) Chuang, T. J.; Hoffman, G. W.; Eisenthal, K. B. *Chem. Phys. Lett.* **1974**, *25*, 201.
(4) Bado, P.; Wilson, K. R. *J. Phys. Chem.* **1988**, *88*, 655.
(5) Alfano, J. C.; Kimura, Y.; Walhout, P. K.; Barbara, P. F. *Chem. Phys.* **1993**, *175*, 147.
(6) Alexander, M. L.; Levinger, N. E.; Johnson, M. A.; Ray, D.; Lineberger, W. C. *J. Chem. Phys.* **1988**, *88*, 6200.
(7) Papanikolas, J. M.; Gord, J. R.; Levinger, N. E.; Ray, D.; Vorsa, V.; Lineberger, W. C. *J. Phys. Chem.* **1991**, *95*, 8028.
(8) Papanikolas, J. M.; Vorsa, V.; Nadal, M. E.; Campagnola, P. J.; Gord, J. R.; Lineberger, W. C. *J. Chem. Phys.* **1992**, *97*, 7002.
(9) Potter, E. D.; Liu, Q.; Zewail, A. H. *Chem. Phys. Lett.* **1992**, *200*, 605.
(10) Liu, Q.; Wang, J-K.; Zewail, A. H. *Nature* **1993**, *364*, 427.
(11) Schriever, R.; Chergui, M.; Unal, O.; Stepanenko, V.; Schwentner, N. *J. Chem. Phys.* **1990**, *93*, 3245.
(12) Schriever, R.; Chergui, M.; Schwentner, N. *J. Phys. Chem.* **1991**, *95*, 6124.
(13) Zoval, J.; Apkarian, V. A. *J. Phys. Chem.* **1994**, *98*, 7945.
(14) Lavrich, D. J.; Buntine, M. A.; Serxner, D.; Johnson, M. A. *J. Chem. Phys.* **1993**, *99*, 5910.
(15) Travers, M. J.; Cowles, D. C.; Ellison, G. B. *Chem. Phys. Lett.* **1989**, *164*, 449.
(16) Lavrich, D. J.; Serxner, D.; Bailey, C. G.; Johnson, M. A. Paper in preparation.
(17) Buntine, M. A.; Lavrich, D. J.; Dessent, D. E.; Scarton, M. G.; Johnson, M. A. *Chem. Phys. Lett.* **1993**, *216*, 471.
(18) Afanas'ev, I. B. In *Superoxide Ion: Chemistry and Biological Implications Vol I*; CRC Press: Boca Raton, FL, 1989.
(19) Symons, M. C. R.; Eastland, G. W.; Denny, L. R. *J. Chem. Soc. Faraday 1* **1980**, *76*, 1868.
(20) Bielski, B. H. *J. Photochem. Photobiol.* **1978**, *28*, 645.
(21) Johnson, M. A.; Lineberger, W. C. In *Techniques in Chemistry*; Farrar, J. M., Saunders, W., Eds.; Wiley: New York, 1988.
(22) Yamdagni, R.; Payzant, J. D.; Kebarle, P. *Can. J. Chem.* **1973**, *51*, 2507.
(23) This differential solvation has been independently determined to be ~0.2 eV in H_2O clusters by a Born−Haber analysis of the following charge-transfer reactions:[24] $O_2 + (H_2O)_n^- \rightarrow O_2^-\cdot(H_2O)_{n-7} + 7(H_2O)$ and $N_2O + (H_2O)_n^- \rightarrow O^-\cdot(H_2O)_{n-5} + 5(H_2O) + N_2$.
(24) Posey, L. A.; DeLuca, M. J.; Campagnola, P. J.; Johnson, M. A. *J. Phys. Chem.* **1989**, *93*, 1178.
(25) Gertner, B. J.; Ando, K.; Bianco, R.; Hynes, J. T. *Chem. Phys.* **1994**, *183*, 309.
(26) Afanas'ev, I. B.; Kuprianova, N. S.; Polozova, N. I. *Int. J. Chem. Kin.* **1983**, *15*, 1045.
(27) Arnold, D. W.; Xu, C.; Neumark, D. M. Submitted to *J. Chem. Phys.*
(28) King, D. S.; Sauder, D. G.; Casassa, M. P. *J. Chem. Phys.* **1994**, *100*, 4200.
(29) Perera, L.; Berkowitz, M. L. *J. Chem. Phys.* **1992**, *96*, 8288.
(30) Perera, L.; Berkowitz, M. L. *J. Chem. Phys.* **1991**, *95*, 1954. Erratum: Perera, L.; Berkowitz, M. L. *J. Chem. Phys.* **1993**, *99*, 4236.
(31) Jorgensen, W. L.; Severance, D. L. *J. Chem. Phys.* **1993**, *99*, 4233.
(32) Dang, L. X.; Garret, B. C. *J. Chem. Phys.* **1993**, *99*, 2972.
(33) Markovich, G.; Giniger, R.; Levin, M.; Cheshnovsky, O. *J. Chem. Phys.* **1991**, *95*, 9416.
(34) Arnold, S. T.; Hendricks, J. H.; Bowen, K. H. In *Reaction Dynamics in Clusters and Condensed Phases*; Jortner, J., Levine, R. D., Pullman, B., Eds.; Kluwer Academic Pub: Dordrecht, 1994; p 37.

JP9507051